LIMNOLOGY
and
OCEANOGRAPHY

ASLO

Limnol. Oceanogr. 64, 2019, 1750–1762
© 2019 Association for the Sciences of Limnology and Oceanography
doi: 10.1002/lno.11149

How effective are tidal marshes as nature-based shoreline protection throughout seasons?

Ken Schoutens,[1]* **Maike Heuner**,[2] **Vanessa Minden**,[3] **Tilla Schulte Ostermann**,[4] **Alexandra Silinski**,[5] **Jean-Philippe Belliard**,[1] **Stijn Temmerman**[1]

[1]Department of Biology, Ecosystem Management Research Group, University of Antwerp, Wilrijk, Belgium
[2]Department Ecological Interactions, Federal Institute of Hydrology, Koblenz, Germany
[3]Department of Biology, Ecology and Biodiversity, Vrije Universiteit Brussels, Brussels, Belgium
[4]Landscape Ecology Group, Institute of Biology and Environmental Sciences, University of Oldenburg, Oldenburg, Germany
[5]GIS and Remote Sensing Section, Institute of Geography Cartography, Georg-August University Göttingen, Göttingen, Germany

Abstract

Nature-based mitigation is increasingly proposed as a strategy to cope with global change and related risks for coastal flooding and erosion. Tidal marshes are known to provide shoreline protection as their aboveground biomass attenuates waves and their belowground biomass contributes to reducing erosion rates. The aim of this study was to quantify how effectively wave attenuation rates and erosion reduction rates are sustained throughout seasons in pioneer tidal marshes in the Elbe estuary (Germany). Changes in hydrodynamics and sediment dynamics were measured during 17 months along three sea-to-land transects of 50 m length. Simultaneously, changes in biomass of the monospecific pioneer vegetation (*Bolboschoenus maritimus)* were measured monthly. This study shows that wave and flow attenuation rates positively correlate with seasonal variations in aboveground biomass, that is: in summer, aboveground biomass and associated wave and flow attenuation rates are highest; while aboveground biomass is washed away during the first storms in autumn or winter, resulting in low wave and flow attenuation rates. Contrastingly, maximum incoming wave heights and flow velocities occur during winter, indicating that wave and flow attenuation is most needed then. However, hibernating root biomass assures low erosion rates in winter, especially at sandy sites. Although wave attenuation by pioneer marshes is highly variable throughout seasons and pioneer marshes alone are not so effective, they might facilitate the survival of higher marshes. Therefore, it is important to conserve or restore a gradual sea-to-land gradient from tidal flats, over pioneer marsh to high marsh to provide nature-based shoreline protection.

Coastal societies are experiencing an increasing risk of flooding and shoreline erosion. Recent storm events including cyclone Haiyan in the Philippines (2013) and hurricanes Irma and Maria in the Caribbean (2017) highlight the vulnerability of coastal societies. As a result of climate change, such extreme storm surges are expected to increase in frequency and intensity over the coming decades (Allison et al. 2009; Bender et al. 2010; Woolf and Wolf 2013). Sea level rise (from the seaward side) and increasing human activities (from the landward side) in the coastal zone amplify the pressure on shorelines even more. Hence, global change necessitates novel, long-term sustainable approaches to protect coasts, deltas, and estuaries against flood and shoreline erosion risks induced by sea level rise, storm surges, and human activities.

Apart from traditional coastal protection by hard structures, such as seawalls and dikes only, nature-based solutions are increasingly proposed as an additional, sustainable shoreline protection strategy (Cheong et al. 2013; Temmerman et al. 2013; Sutton-Grier et al. 2015). In this context, the conservation or creation of tidal marsh ecosystems between the sea and the hard defenses in front of coastal communities provides protective functions (Costanza et al. 2008; Duarte et al. 2013; Temmerman and Kirwan 2015) such as wave attenuation (Ysebaert et al. 2011; Yang et al. 2012; Möller et al. 2014), sediment stabilization and accretion (French 2006; Mudd et al. 2010; Kirwan and Megonigal 2013; Ma et al. 2014), and storm surge attenuation (Wamsley et al. 2010; Smolders et al. 2015; Stark et al. 2015; Van Coppenolle et al. 2018). Apart from flood and erosion risk reduction, tidal marsh ecosystems provide other valuable ecosystem services, including water quality regulation, carbon sequestration, contribution to fisheries production and recreation (Barbier et al. 2011), which is why nature-based solutions have multiple benefits in addition

*Correspondence: ken.schoutens@uantwerpen.be

Additional Supporting Information may be found in the online version of this article.

to traditional hard structures (Turner et al. 2007; Narayan et al. 2016, 2017; Arkema et al. 2017). Furthermore, combining nature-based and hard defense structures, e.g., by restoring or conserving tidal marshes in front of dikes or breakwaters forms a cost-effective measure due to the self-sustaining character of tidal marshes which have the ability to adapt to sea level rise by sediment accretion (Temmerman and Kirwan 2015; Kirwan et al. 2016).

Marsh vegetation exerts friction to the water motion and thereby attenuates currents and waves (Yang et al. 2012; Möller et al. 2014; Carus et al. 2016; Vuik et al. 2016). Even narrow fringes at the seaward edge of dikes have a stabilizing effect since the majority of incoming wave height, and thereby wave energy, is reduced in the first few meters of the pioneer marsh (80% over <50 m, Ysebaert et al. 2011; 20–40% over 12 m, Silinski et al. 2017). Although water depth on marshes is higher during storm surge conditions and the rate of wave attenuation is known to be reduced with greater water depth (Gedan et al. 2011; Yang et al. 2012), flume studies under simulated storm conditions show that up to 60% of wave height reduction can be attributed to marsh vegetation (Möller et al. 2014). Reduced hydrodynamic forces decrease the risk of sediment erosion and stimulate sediment deposition on the marsh surface (Mudd et al. 2010). In the pioneer zone (i.e., the gradually sloping transition zone between bare tidal flats and densely vegetated marshes, which is vegetated by pioneer plant species), however, vegetation density-dependent processes such as turbulence around single shoots or increased current speed around vegetation patches might also cause local scouring or erosion (Bouma et al. 2009; Silinski et al. 2016*b*).

The efficiency of wave attenuation and erosion risk reduction by vegetation depends on the plant morphological traits (Barbier et al. 2008; Tempest et al. 2015). Both field and flume studies showed that higher standing biomass, higher shoot densities, and higher stiffness enhance wave attenuation (Bouma et al. 2010; Ysebaert et al. 2011; Silinski et al. 2017). Most studies focused on the effects of aboveground biomass on wave and current attenuation, while the role of belowground biomass in erosion risk reduction has long been neglected (Bouma et al. 2014). Recently, a mesocosm experiment showed that the presence of a belowground root network can enhance the stability and reduce the erodibility of the sediment (Wang et al. 2017). Additionally, field and flume studies emphasize the function of belowground biomass for reducing erosion of the sediment surface of tidal marshes (Coops et al. 1996; Chen et al. 2012; Francalanci et al. 2013). Even after harsh storm conditions in winter, the marsh surface has been observed to remain stable (Spencer et al. 2015).

Most above-mentioned field studies on wave attenuation and erosion risk reduction by tidal marshes are based on observations during relatively short periods in summer when vegetation biomass is maximal. However, in temperate climate regions, where tidal marsh vegetation depicts seasonal growth cycles, these results cannot be extrapolated to a full year. In particular, in regions where plants die back in winter and standing biomass diminishes (e.g., Charpentier and Stuefer 1999; Coulombier et al. 2012; Silinski et al. 2016*a*), marshes may be less effective in wave and erosion risk reduction in winter. In many cases, the winter period is associated with a higher storm activity. Historical records of storm surges along the coast of northwest Europe show that most severe events occurred during winter (e.g., Saint Marcellus flood 1219 and 1362, North Sea flood 1953, but also more recent floods such as cyclone Xavier in 2013 and cyclone Burglind in 2018) which coincide with most historical dike failures (van Baars and van Kempen 2009) as a result of wave overtopping (Stanczak et al. 2007; Morris et al. 2009; Steendam et al. 2011; Le Hai and Verhagen 2014). Therefore, existing studies on wave attenuation in marshes during summer peak-biomass conditions give an overestimation of year-round wave attenuation capacity of temperate zone tidal marshes.

The aim of this article is to quantify the impact of seasonal differences of both aboveground and belowground tidal marsh plant biomass on wave attenuation and erosion-sedimentation rates. This research was conducted in a temperate-zone tidal marsh in the Elbe estuary (Germany) during a 17 months period from December 2015 to April 2017. We address the following research questions:

a. Are wave attenuation rates (i.e., the reduction of wave height with distance traveled through the marsh) (1) directly related to temporal (seasonal) changes in aboveground biomass and (2) lowest in winter when aboveground biomass is minimal? In other words, how effective is the marsh in attenuating waves in winter?
b. To what extend is the sediment stabilizing effect induced by the vegetation reduced in winter compared to summer? Are erosion rates on the marsh still lower compared to the adjacent tidal flat as a result of stabilization by belowground hibernating biomass?

Methods

Study sites

Field work was conducted in the Elbe estuary (Germany, 53° 47′ N, 9° 22′ E) which is one of the principal waterways in Western Europe of high economic and natural value. It is both geomorphologically and ecologically comparable to other NW European estuaries. Intertidal marsh sites were chosen based on the following criteria: (1) presence of monospecific stands of *Bolboschoenus maritimus* (L.) Palla, which is the dominant pioneer species in brackish marshes in NW European estuaries; (2) continuous marsh edge, parallel to the estuarine subtidal channel; (3) gently sloping transition between bare tidal flat and marsh (slope ≤ 1°); and (4) absence of obstructions (e.g., riprap) on the seaward side of the marsh (Fig. 1). The halophyte *B. maritimus* forms clonal stands of fast growing aboveground shoots, which can reach stem heights of up to 2 m (Silinski et al. 2017) and which die off and are flushed away in

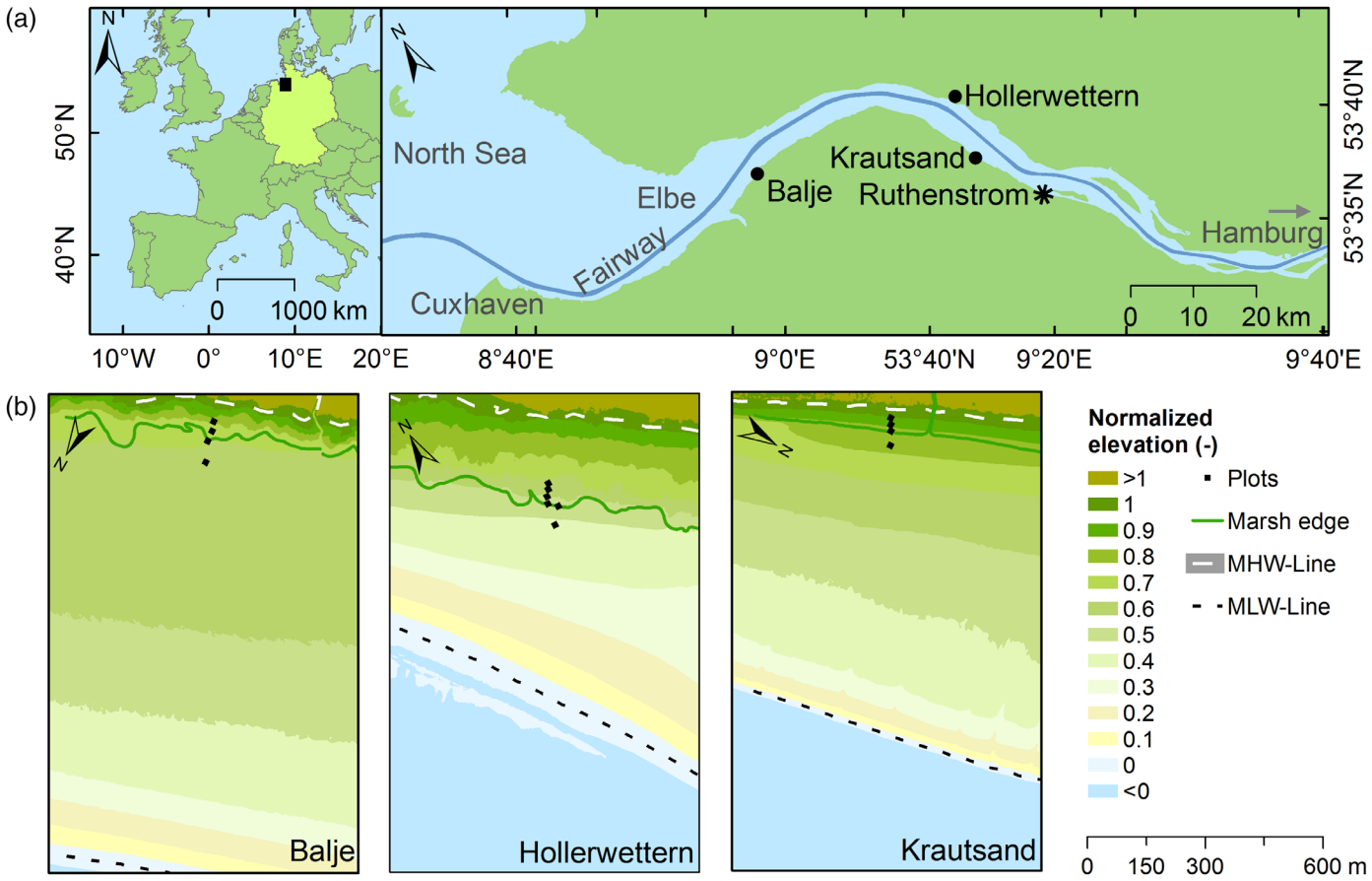


Fig. 1. Location and characteristics of the study sites along the Elbe estuary in Germany. (**a**) Location of the Elbe estuary in Europe and of the three study sites: Balje, Hollerwettern, Krautsand together with Ruthenstrom weather station. (**b**) The elevation maps for all sites showing the marsh edge and width of the tidal flat as well as the mean low and high water level (MLW and MHW). The elevations are normalized by tidal range as (Elevation − Mean low water)/(Mean high water − Mean low water). [Color figure can be viewed at wileyonlinelibrary.com]

autumn and winter (*see* Supporting Information). Belowground tubers and a dense root network ensure the survival in winter and the regrowth of new shoots in spring. Three sampling sites (Balje: 53°51′23.5″N, 9°4′9.2″E; Hollerwettern: 53°49′55.5″N, 9°22′17.4″E; and Krautsand: 53°46′32.3″N, 9°22′5.9″E) were selected in the brackish part of the estuary. The salinity ranges from 0.3 PSU to 4.0 PSU and the semidiurnal tidal range is on average 2.8 m (1.6 m during neap tide and 3.8 m during spring tide) in all three sites (2015–2017). Mean freshwater discharge of the Elbe (1926–2014) is 712 $m^3\ s^{-1}$ ranging from 560 $m^3\ s^{-1}$ in summer to 866 $m^3\ s^{-1}$ in winter (Strotmann 2014). Suspended sediment concentration varies as a positive function of freshwater discharge between 0.3 $kg\ m^{-3}$ and 1.0 $kg\ m^{-3}$ (Bundesanstalt für Gewässerkunde 2014). The wind climate is shown in the Supporting Information, and it is characterized by winds predominantly blowing from the southwest (DWD Climate Data Center 2019).

Monitoring plots

At each study site, a cross-shore transect of 50 m length, starting at the bare tidal flat 30 m in front of the seaward marsh edge and reaching 20 m into the marsh, was set up. Elevations ranged between −1.0 m MSL (relative to local mean sea level) on the tidal flat and −0.2 m MSL in the marsh at Balje, between −1.5 m MSL and −0.5 m MSL at Hollerwettern, and between −0.6 m MSL and 0.0 m MSL at Krautsand. Within the marsh, the measurement plots were set up at an interval of 10 m (Fig. 2). At each plot wave heights, sedimentation-erosion rates, sediment properties, and vegetation biomass (within the marsh over a 15 m stretch parallel to the marsh edge) were monitored.

Measurements

Hydrodynamics

Waves

Wave heights were measured continuously over 17 months from December 2015 until April 2017. We deployed three pressure sensors along the transect at each of the three sites (i.e., nine wave sensors in total), i.e., at the marsh edge, 10 m into the marsh and 20 m into the marsh. Wave attenuation on the tidal flat (representing nonvegetated conditions with only bed friction) was measured during three measurement campaigns of 1–2 weeks in March, August, and January by deploying

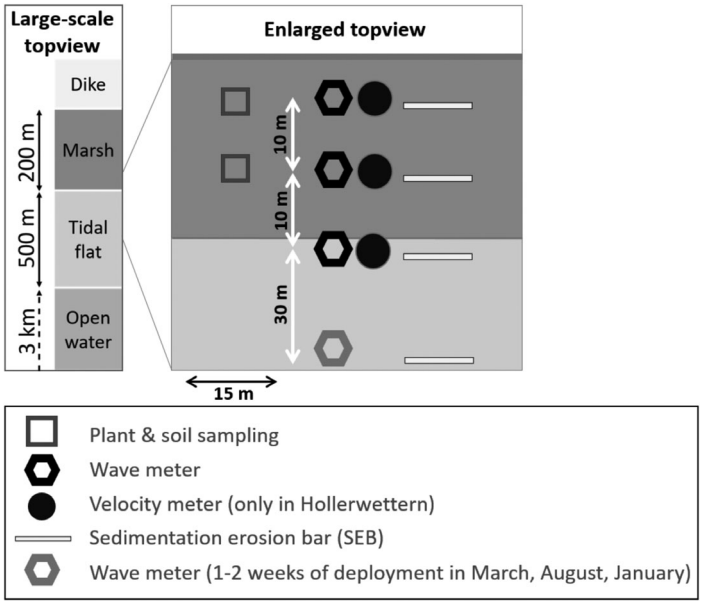


Fig. 2. Top view of the monitoring setup along the cross-shore transect at each of the three sites. At each plot, wave heights, sedimentation-erosion rates, sediment properties, and vegetation biomass were measured.

an additional pressure sensor 30 m from the marsh on the tidal flat (Fig. 2). The automated pressure sensors (P-Log3021-MMC, Driesen & Kern) sampled at a frequency of 8 Hz. Pressure data were then converted into water surface elevation with a Matlab routine. Raw data (absolute pressure) were first corrected for atmospheric pressure (DWD Climate Data Center, Ruthenstrom: 7.0 m above ground surface) and then converted into meters of water. Resulting water levels were corrected for depth-dependent pressure attenuation based on linear wave theory (Dalrymple and Dean 1991). Next, a low-pass filter with a cutoff frequency of 0.002 Hz was used to separate the tidal signal (i.e., slow water level changes with a semidiurnal period) from the wave signal (i.e., fast water level fluctuations with a period in the order of seconds). Waves resulted from both wind-generated and ship-generated waves; however, no distinction was made for further analyses. From the processed wave data, we calculated significant wave height (H_s, mean of the highest third of recorded waves) and $H_{1/100}$ (mean of the highest 1% of recorded waves) over 10 min time intervals. The relative wave attenuation rate (R) was calculated as $R = (H_{in} - H_{10m})/H_{in} \times 100$ (%), where H_{in} are the incoming significant wave heights at the seaward edge of the *B. maritimus*-zone and H_{10m} are the significant wave heights at 10 m into the *B. maritimus*-zone.

Flow velocity

Flow velocities were measured with three ADVs (Acoustic Doppler Velocity sensors, Nortek) at one of the transects (Hollerwettern, Figs. 1, 2). They were positioned horizontally with the central beam at 0.10 m above the sediment surface. Raw data were filtered for beam correlations below 70% after which the planar velocity was calculated as $U = \sqrt{u^2 + v^2}$ (m s^{-1}) with u and v being the two horizontal flow velocities (m s^{-1}) perpendicular to each other. Flow attenuation rate was calculated in the same way as the wave attenuation rate (see above). Wave and flow data were compared with hourly wind data of the Ruthenstrom station (Fig. 1) obtained from the German Meteorological Office (DWD Climate Data Center 2019).

Sediment properties and dynamics

The erosion-sedimentation rates at each plot along the transects were monitored next to the pressure sensors (Fig. 2), so that elevation changes could be correlated to wave heights. By monitoring elevation changes on the tidal flat and in the marsh, we could compare elevation changes without and with presence of belowground biomass. Monthly measurements were conducted with sedimentation erosion bars (SEBs), each consisting of two vertically positioned poles 2.0 m apart and inserted 1.0 m into the sediment bed, on top of which a horizontal bar was placed as reference level to measure sediment surface elevation changes (van Wijnen and Bakker 2001; Nolte et al. 2013; Silinski et al. 2016*a*). The SEBs were installed parallel to the marsh edge and for each SEB, the sediment surface elevation was measured at 10 replicate locations at 10 cm horizontal distance intervals with a vertical accuracy in the order of 1.5 mm. Additionally, site-specific sediment characteristics were quantified monthly on three replicate samples per plot. Samples from the sediment bed were taken with a Kopecky ring (4.6 cm in diameter and 5.2 cm high) and used to determine dry bulk density and water contents (after drying at 70°C for 72 h). Next, the same samples were used to perform grain size analyses with a Mastersizer 2000 (Malvern) after a combined H_2O_2 and HCl treatment to remove organic compounds and disperse aggregates. Organic matter content was determined with loss on ignition, i.e., by ashing the samples at 550°C for 6 h.

Plant biomass

Biomass of *B. maritimus* was measured monthly from February 2016 until February 2017. Aboveground biomass was sampled by clipping all shoots in 0.2 m × 0.2 m quadrants (if needed this was repeated until a minimum of 20 shoots was reached). To derive the aboveground biomass per square meter, shoot densities were determined per plot by counting the number of shoots (i.e., dead and living) within three permanent quadrats of 0.4 m × 0.4 m. Belowground plant biomass was quantified three times, i.e., in April, August, and December 2016 by taking three replicate soil cores per plot with a diameter of 0.1 m up to a depth of 0.45 m. After rinsing, biomass was quantified as dry weight (drying at 70°C for 72 h) per square meter of soil.

Data analyses

All analyses were performed in R 3.3.1. (R Core Team, 2016) and significance was assumed at $p < 0.05$ for all tests. Prior to

statistical analyses, the data were checked for normality based on visual inspection of histograms and normal Q-Q plots. If needed, transformations (logarithmic or square root) of the data were applied to approximate normal distribution. We explored if temporal variations in significant wave height were correlated with wind speed (hourly intervals) and sedimentation-erosion rates (monthly intervals). Wind directions were taken into account by making the correlation for different classes of wind direction (every class represents 45°, e.g., the "North" direction corresponds to all wind speeds ranging in between 337.5° and 22.5°). We tested correlations between wave attenuation rate, water depth (temporal, 10 min intervals), and aboveground biomass (spatial and temporal, monthly intervals) as well as between sedimentation-erosion rates (temporal, monthly intervals) and aboveground biomass (temporal, monthly intervals). For correlations with wave attenuation rates, we used the non-parametric Spearman's rank coefficient (rho, i.e., ρ). The Pearson correlation coefficients (r) were calculated for all other correlations. The variables tested for correlation were recast where necessary for a matter of data consistency. The temporal and spatial effect of aboveground biomass on wave attenuation was explored by multiple linear regression taking into account the sites and time of the year (month). Visualizing the wave, wind, and current velocity data by applying a simple moving average (over one tide) reveals the potential seasonal trends in the time series. Comparisons of the mean flow and wave attenuation rates in summer (defined as the period May–August) and winter (defined as the period December–March) were performed using a Wilcoxon signed-rank test. Local polynomial regression (LOESS) was applied to the monthly measurements (time series) of aboveground biomass and sedimentation-erosion rates.

Results

Incoming waves and flow velocities at the marsh edges

Wave heights entering the *B. maritimus* vegetation are shown throughout the seasons from December 2015 until May 2017 (Fig. 3). Over the whole monitoring period, the average significant wave height was 0.09 m and the average maximum wave height was 0.30 m (Table 1). In winter, time periods were measured with significant wave heights up to 1.0 m and maximum wave heights up to 1.5 m (based on the 10 min interval data). These extremes were observed during three distinct tides (26 December 2016, 04 January 2017, and 12 January 2017) and coincided with high-wind speeds coming from the west and northwest (Fig. 3). Overall, Hollerwettern was the most exposed site with longer and more frequent inundation periods and Krautsand the least exposed site as a result of its higher elevation (Table 1). Median wave heights are comparable between the three sites. Gaps in the data resulted from removing the wave or ADV sensors from the field to prevent frost damage, from battery failure or from noninundated periods.

Highest flow velocities coincided with highest wind speeds (from December 2016 to mid-March 2017). Wind speeds and significant wave heights were well correlated with the longest wind fetch directions per site, i.e., NW directions in Balje; Spearman's $\rho = 0.60$; $p < 0.05$, SW, NW and SE directions in Hollerwettern; Spearman's $\rho = 0.74$, 0.64, and 0.50, respectively; $p < 0.05$ and NW directions in Krautsand; Spearman's $\rho = 0.70$; $p < 0.05$.

Wave and flow attenuation over the marsh transects

The seasonal effect of vegetation as physical buffer for waves is clearly demonstrated by the change in wave attenuation rates from winter to summer and back to winter (Fig. 4). Over a 10 m stretch of *B. maritimus* vegetation, wave heights were attenuated up to 50% in summer while in winter a maximum attenuation of only 10% was reached. The wave attenuation rate decreased with increasing water depth over the course of individual tidal cycles ($F_{21;37,576} = 1383$, $R^2 = 0.44$, $p < 0.05$). Moreover, at water depths higher than 1.5 m, no seasonal change in wave attenuation rate was observed. In Balje, wave attenuation rates were >10% higher than in the other two sites during the whole year. Although there was a clear summer-peak of wave attenuation rate in all sites, the decline in Balje and Hollerwettern started in August until September, while in Krautsand wave attenuation rate only decreased in December 2016. Wave attenuation rates within the marsh during winter are in the same range as on the bare tidal flat. Here, wave attenuation rates stay below 10% all year long (based on short term measurement periods of 1–2 weeks in March and August 2016 and January 2017).

Flow attenuation rates were significantly higher in summer and spring situations (>15% higher attenuation rates) than during the two winter periods (Fig. 5). Apart from the seasonal differences, it should be mentioned that there might be some interannual differences too.

Sediment characteristics and dynamics

The changes in sediment surface elevation varied between sites and between the tidal flat and the tidal marsh. Median grain sizes are all <125 μm and differ between the sites (Fig. 6b). Balje has the finest grain size (34% sand, 63% silt, and 3% clay) with mainly silt while Krautsand (69% sand, 30% silt, and 1% clay) is dominated by sandy sediments and Hollerwettern (56% sand, 42% silt, and 2% clay) has an intermediate grain size distribution. Over the entire measurement period, the tidal flat in Krautsand experienced periods of severe erosion (Fig. 6a), in particular during the winter of 2016. In Hollerwettern, there was some erosion in winter, but a net sedimentation was observed over the entire measurement period. In contrast, elevation changes on the tidal flat in Balje were limited. In the tidal marsh, the patterns for Hollerwettern and Balje are comparable to the ones on the tidal flat with an overall net sedimentation. In Krautsand, however, a strong sedimentation up to >15 cm was observed. During the field campaigns, benthic diatoms were only observed on the tidal flat in Balje and Hollerwettern. Significant incoming wave

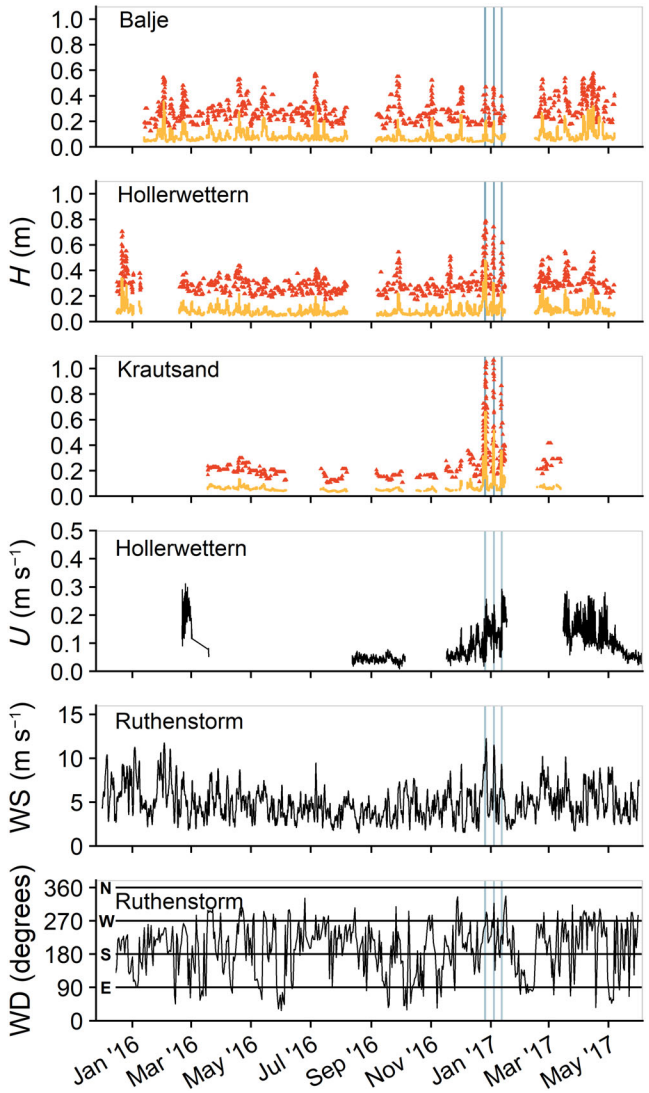


Fig. 3. Significant wave height (H_s, yellow squares) and $H_{1/100}$ (mean of the highest 1% of recorded waves, red triangles) are represented as the moving average over one tide and are shown for the three study sites. Planar flow velocity (U; m s^{-1}) at the marsh edge in Hollerwettern, wind speed (WS; m s^{-1}) and wind direction (WD; degree) at the weather station Ruthenstrom are represented as a moving average (calculated over 3 h from 10 min interval flow data and calculated over 24 h from hourly interval wind data). These data are shown from December 2015 until May 2017. Storm days in winter are marked with vertical (blue) lines. [Color figure can be viewed at wileyonlinelibrary.com]

heights increased erosion risk in Krautsand ($F_{1,74} = 15.34$, $p < 0.05$), but no effect was found for Hollerwettern and Balje ($F_{1,102} = 2.41$, $p > 0.05$ and $F_{1,87} = 0.49$, $p > 0.05$, respectively). Wave attenuation and elevation change were only correlated in Krautsand (Spearman's $\rho = 0.53$, $p < 0.05$).

Plant biomass

Aboveground plant biomass was lowest during the winter months with only small dead shoot stumps remaining (<50 g m^{-2}) (Fig. 7a). The biomass increased rapidly in May and growth continued until peak biomass (700–900 g m^{-2}) was reached in mid-August. Hollerwettern showed a slightly lower peak biomass (500–700 g m^{-2}). After peak biomass was reached in summer, it started to decrease earlier in Balje and Hollerwettern (August) while the high biomass in Krautsand remained longer before the decrease started (September–October). Concerning the belowground biomass, no significant temporal or site specific differences were observed (Fig. 7b). Closer to the marsh edge, belowground biomass is consistently lower compared to 20 m into the marsh.

Relation between biomass and wave attenuation and erosion-sedimentation rates

Aboveground biomass correlated positively with wave attenuation rates at all sites (Fig. 8). Furthermore, from this figure, it can be seen that observations during periods of low-water depths lie above the regression lines and observations during periods of higher water depths lie mainly below the regression lines. Multiple linear regression shows that wave attenuation rate is explained by aboveground biomass (partial $R^2 = 0.42$) and there is indeed an important effect of water depth (partial $R^2 = 0.28$) ($F_{5,84} = 42.94$, $p < 0.05$, $R^2 = 0.70$). The friction effect of the bed topography is shown by the intercept which is similar in Balje and Hollerwettern and slightly higher in Krautsand. No relation was found between aboveground biomass and sedimentation-erosion rates ($R^2 = 0.02$, $p > 0.05$) nor between belowground biomass and wave attenuation rates ($R^2 = 0.03$, $p > 0.05$).

Discussion

Tidal pioneer marshes in the temperate climate regions may lose much of their aboveground biomass in winter which temporarily reduces the efficiency of the marsh for shoreline

Table 1. Overview of the main hydrodynamic variables per site over the entire monitoring campaign measured at the marsh edge of each respective study site; mean inundation depth (I_{depth}, m), mean inundation time per tide (I_{time}, min), percentage of time inundated (I_{perc}, %), median of the significant wave heights (H_s, m), median maximum wave height ($H_{1/100}$, m), highest wave (H_{max}, m), median planar flow velocity (U, m s^{-1}), and normalized elevation at the marsh edge (Z_{norm}).

Site	I_{depth} (m)	I_{time} (min)	I_{perc} (%)	H_s (m)	$H_{1/100}$ (m)	H_{max} (m)	U (m s^{-1})	Z_{norm}
Balje	0.70	263	35	0.09	0.15	0.91	0.11	0.66
Hollerwettern	1.14	374	50	0.10	0.17	1.28	0.09	0.50
Krautsand	0.43	177	21	0.09	0.16	1.72	0.07	0.83

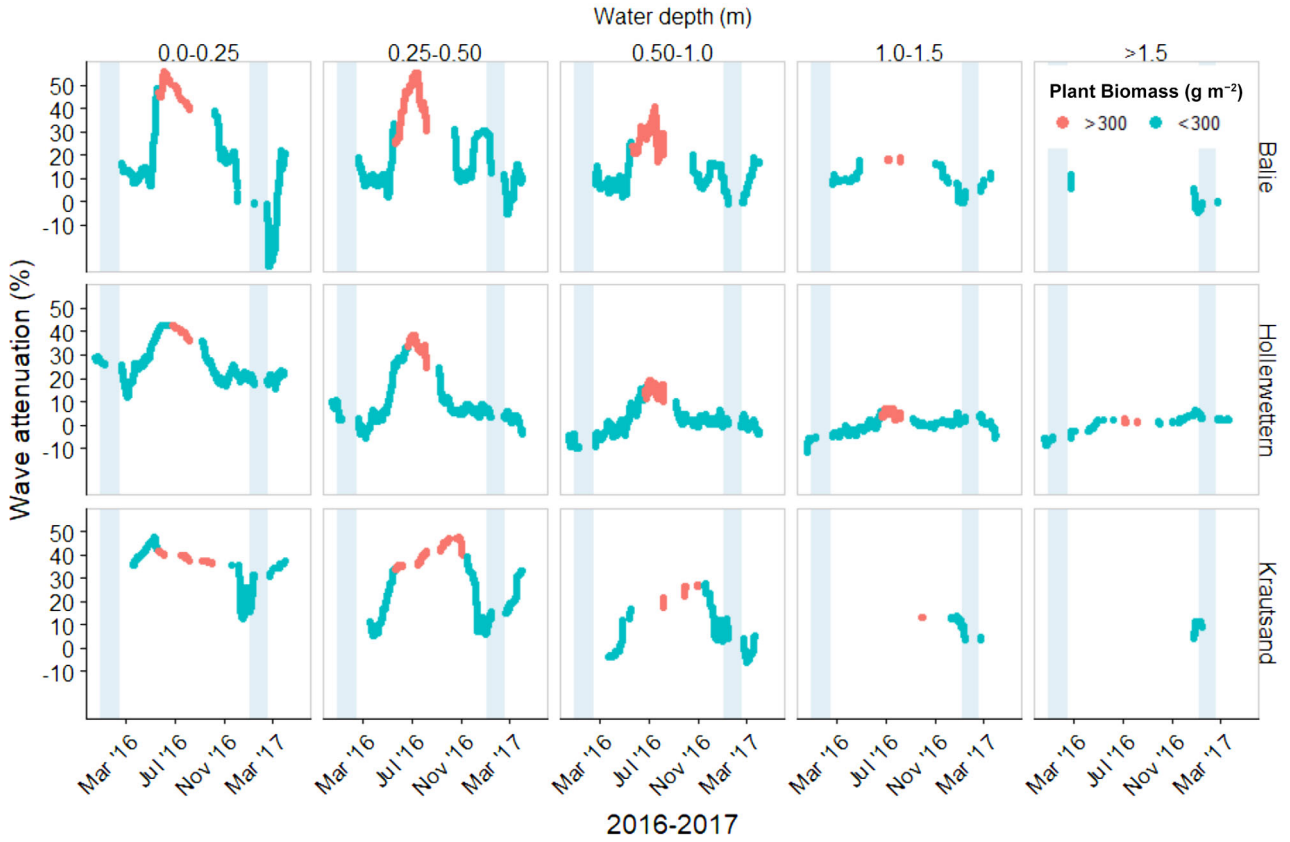


Fig. 4. Wave attenuation rate over 10 m of *B. maritimus* at the three study sites from winter 2015 to spring 2017 for different water depths during the tidal inundated periods. Lines represent a moving average of the wave attenuation rate (calculated over windows of 3 d, based on 10 min interval data) and red colors represent the period of high standing biomass (>300 g m^{-2}, *see* Fig. 7) while blue colors represent the low biomass conditions during winter (<300 g m^{-2}). The periods indicated by blue background are periods of frost and potential ice formation, which is likely to affect the wave data and therefore these periods were excluded from the data analysis. [Color figure can be viewed at wileyonlinelibrary.com]

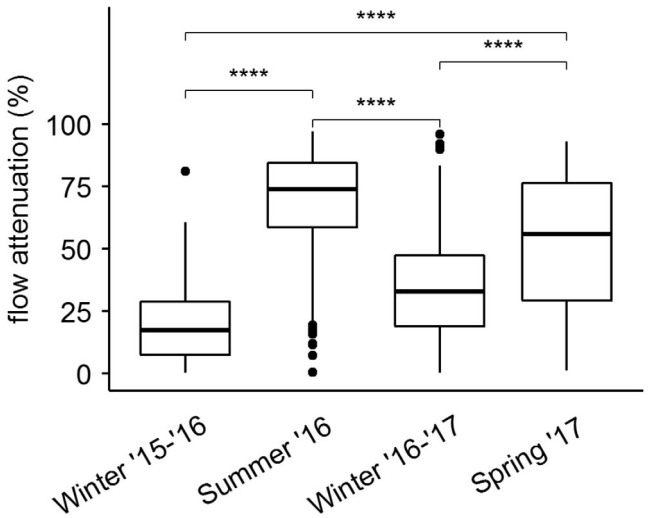


Fig. 5. Flow attenuation rates over 10 m of *B. maritimus* in Hollerwettern. The boxplots represent the summer and winter periods (10 min intervals). Comparisons of the medians were performed using a Wilcoxon rank sum test with the asterisks representing the significance level of α = 0.001.

protection. Although the general processes of wave attenuation (Ysebaert et al. 2011; Yang et al. 2012; Möller et al. 2014; Silinski et al. 2017) and erosion reduction (Chen et al. 2012; Francalanci et al. 2013; Wang et al. 2017) by tidal marshes are well studied, studies are mostly done under peak-biomass (summer) conditions while studies under low biomass (winter) conditions are sparse (Coulombier et al. 2012; Spencer et al. 2015; Vuik et al. 2016). In this study, we quantify seasonal changes in wave attenuation rates and sedimentation-erosion rates in pioneer marsh vegetation. We showed that the wave attenuation capacity of the pioneer tidal marsh vegetation is strongly reduced in winter, when incoming wave heights are highest during storms, and hence when marsh-induced shoreline protection is most needed. In contrast, sediment stabilization is maintained due to the presence of hibernating belowground biomass especially at sandy sites.

At our field sites, strongest hydrodynamic conditions (both significant wave heights and flow velocities) occur during winter. This is a combined effect of higher wind speeds (Fig. 3) and higher river discharge (560 $m^3 s^{-1}$ in summer vs. 866 $m^3 s^{-1}$

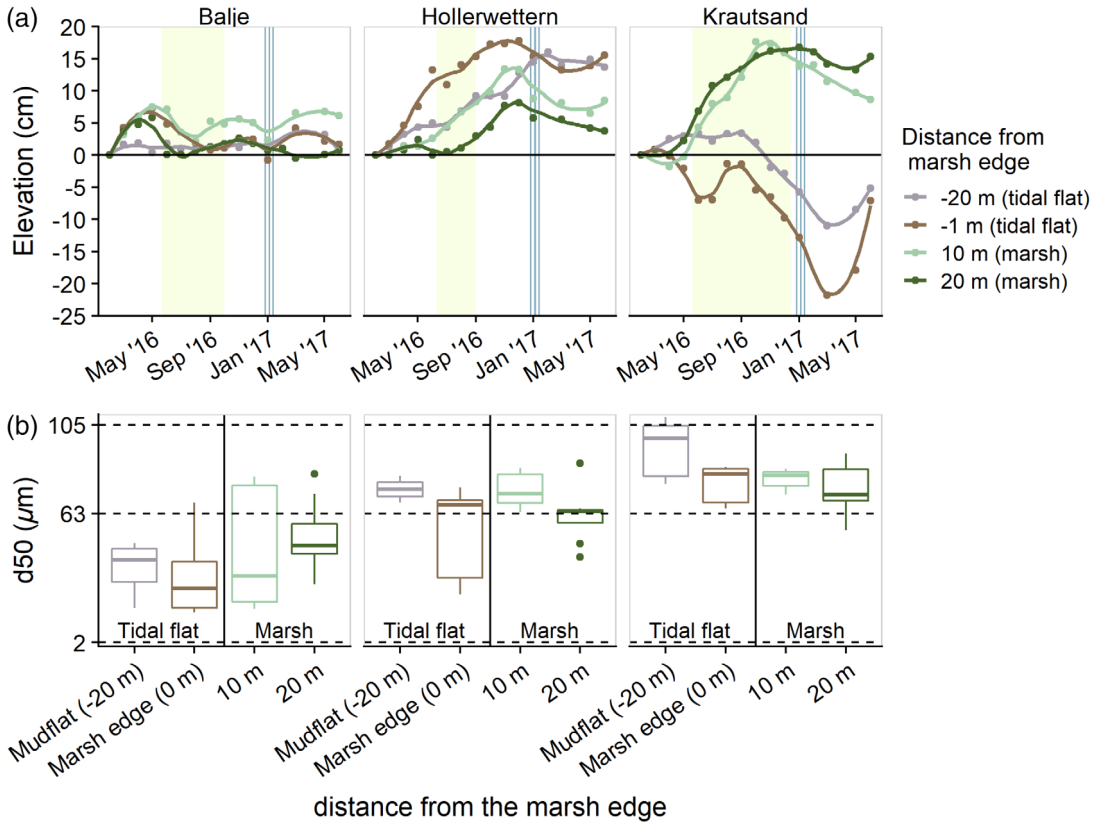


Fig. 6. (**a**) Elevation (cm) relative to the first measurement at the three study sites from February 2016 to June 2017 for different distances from the marsh edge. Negative distances are on the tidal flat and positive distances are at the landward side of the marsh edge (monthly measurements; n = 10). The green shaded areas delineate the period of high biomass (>300 g m^{-2}, see Fig. 7). Storm days in winter are marked with vertical blue lines. (**b**) Median sediment grain size (d50 in μm) for the three sites and for different distances from the marsh edge (n = 9). [Color figure can be viewed at wileyonlinelibrary.com]

in winter) (Bundesanstalt für Gewässerkunde 2014; Kappenberg et al. 2016). Along the coast of northwest Europe, the most severe storm events and dike failures typically occurred during winter (see above-mentioned historical records). This highlights that shoreline protection in northwest Europe is most needed during the winter period. Although Krautsand has the lowest median wave heights throughout the year (Table 1), highest wave heights were recorded here during three distinct storm tides in the winter of 2016–2017. This can be explained by the morphological characteristics of the tidal flat and marsh. It has an overall higher elevation as compared to the two other study sites, which reduces the inundation depth and therefore limits the wave heights during normal tides. However, the concave cross-sectional shape of the tidal flat creates a short and steep slope right in front of the marsh edge, which during storm surge conditions (i.e., higher water depths) allows the landward propagation of higher waves (*see* Supporting Information on cross-sectional profiles of the three study sites).

The wave and flow attenuation rates that are reported in the literature, and that were typically measured during summer peak-biomass conditions (Leonard and Croft 2006; Ysebaert et al. 2011; Silinski et al. 2017), are in the same range as our measurements for summer peak biomass. However in the present study, wave and flow attenuation rates were measured throughout the season. In contrast to the rates in summer, wave and flow attenuation rates were almost negligible in winter (Figs. 4, 5). Regarding flow attenuation rates, these findings are supported by the measurements done by Carus et al. (2016) who covered two sites along the brackish part of the Elbe and measured flow attenuation rates in *B. maritimus* both under unvegetated (April) and vegetated (August) conditions. These contrasting attenuation rates between summer and winter emphasize the necessity to evaluate the shoreline protection capacity of tidal marshes throughout a full yearly cycle, taking into account the low-biomass periods of the pioneer zone during winter. In addition, wave attenuation rates decrease with water depth (Figs. 4, 8) and when water depths exceed 1.5 m the attenuation effect of pioneer marshes is negligible even during the summer season with peak biomass. This observation highlights the importance of wave attenuation in higher marshes landwards of the pioneer zone. Even though pioneer marshes lose their wave attenuation capacity during deeper inundation periods, it may be expected that the higher marshes will take over this function.

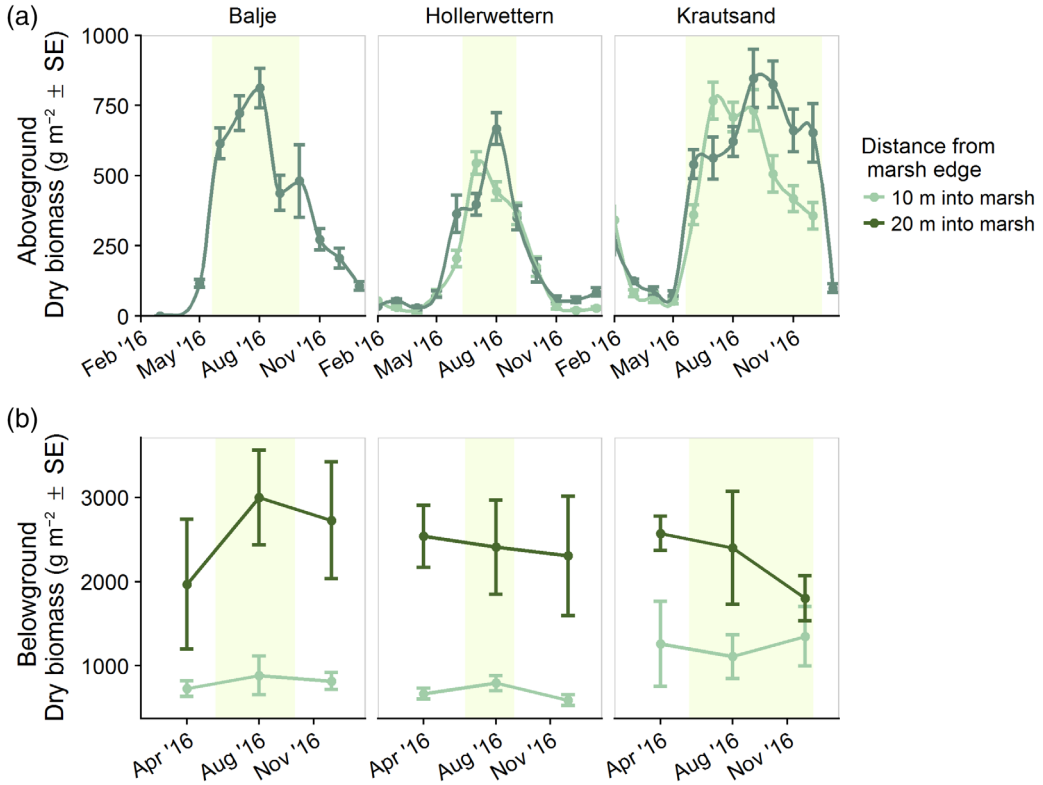


Fig. 7. Time series of (**a**) aboveground (n >20) and (**b**) belowground (n = 3) dry biomass/m^2 per site in the period between February 2016 and January 2017 for two distances in the marsh. The green shaded area indicates the period of high aboveground biomass (>300 g m^{-2}). Data of aboveground biomass at 10 m into the marsh in Balje are left out of the graph because *B. maritimus* was dominated by another species (*Schoenoplectus tabernaemontani*) after 2–3 months in the growing season of 2016. [Color figure can be viewed at wileyonlinelibrary.com]

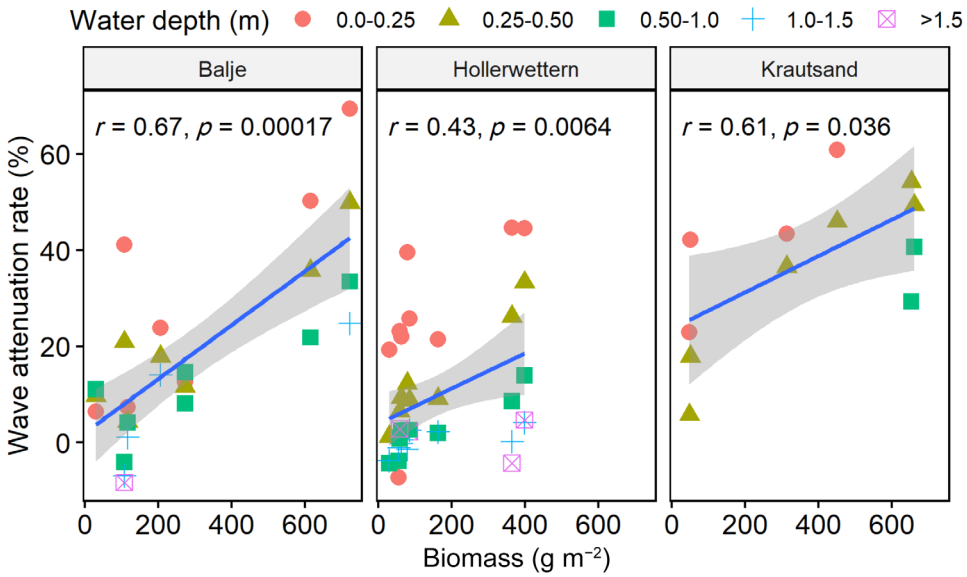


Fig. 8. The relation between aboveground plant biomass (g m^{-2}) and the wave attenuation rate (%) (average calculated over 1 week time period, i.e., 5 d before until 1 d after sampling of the biomass) for the three sites. Linear regression lines with confidence intervals (95%) are displayed. The different symbols refer to water depths (m) at which the wave attenuation rate was measured. [Color figure can be viewed at wileyonlinelibrary.com]

Under average inundation depths, the wave attenuation rates reflect the seasonal changes in aboveground biomass as they increase rapidly at the start of the growing season beginning of May, reaching a peak in August, and decreasing simultaneously at the end of the growing season (compare Figs. 4, 7). At the marsh sites of Balje and Hollerwettern, the aboveground biomass starts to decrease already directly after August from September to December (Fig. 7). At the marsh of Krautsand, the aboveground biomass is not washed away immediately in autumn and thus wave attenuation rates remain high in autumn and only drop after the first winter storms have removed this biomass (i.e., after the stormy days of 26 December 2016, 27 December 16, 04 January 2017, and 12 January 2017; compare Figs. 3, 7). The reason why biomass is washed away later in Krautsand as compared to the other two marsh sites, is probably because of the higher location of the marsh edge, i.e., causing a shorter inundation time and lower inundation frequency (Table 1) in combination with low incoming wave heights during fall (Fig. 3) which allows the decaying vegetation to remain without being washed away. Only when significant wave heights start to increase (December 2016–January 2017 at Krautsand), the aboveground biomass starts to decrease (Figs. 3, 7). This suggests that waves play a role in breaking off the decaying vegetation and subsequently washing away the broken stems (Vuik et al. 2018). As a result, biomass removal happens earlier at sites exposed to stronger wave conditions.

Although aboveground biomass of the pioneer vegetation is washed away, the belowground biomass persists throughout winter (Fig. 7). The role of the belowground biomass for reducing erosion risk is not straightforward to interpret from our results as the biomass-effect seems to interact with other variables that influence the erosion-sedimentation rates. The sediment composition seems to be an important variable. At the more sandy site (Krautsand), the roots within the marsh seem to protect the sediment from erosion during the winter period, in contrast to the eroding unvegetated tidal flat (Fig. 6). However, this discrepancy between eroding tidal flat and protected marsh was not visible at the other two sites which are characterized by finer sediments that are expected to be more cohesive and thus less vulnerable to erosion by hydrodynamic forcing (Hjulstrom 1935). Furthermore, the presence of benthic diatoms probably enhanced the sediment stability in the latter two sites (Sutherland et al. 1998). For these two sites, the hydrodynamic forcing might not have been strong enough to see any response. This suggests that especially in areas with sandy sediment, which typically has a noncohesive nature and is less prone to developing a diatom film, the presence of belowground biomass contributes most to increased sediment cohesion and hence to erosion reduction (Vannoppen et al. 2017). Although the stabilizing effect of belowground biomass for soil erosion reduction in terrestrial landscapes is known (De Baets et al. 2008; Francalanci et al. 2013; Vannoppen et al. 2015), the functional role in reducing erosion throughout all seasons has not been described yet.

We highlight that our study focused on pioneer tidal marshes, i.e., at the seaward edge of marshes (first 20 m), where in temperate climate zones the aboveground decaying biomass is washed away in winter due to incoming waves and tidal currents. In contrast to pioneer tidal marshes, we observed that the aboveground biomass in the more landward and higher portions of the studied marshes (>100 m landwards) remains relatively unchanged during winter. Although the vegetation in the high marshes deteriorates, not all dead stems are flushed away and a considerable part of the aboveground biomass remains standing even during winter. This might be the combined consequence of lower wave heights and less frequent inundation as a result of the higher elevation and friction with the bottom and a change in species composition. For instance, the higher marshes in this brackish part of the Elbe are often dominated by *Phragmites australis*, which might have a different response to hydrodynamic forces. When marshes are broad and high enough, the wave attenuation function of the whole marsh is thus not necessarily lost in winter. Furthermore, the low pioneer tidal marshes sustain erosion risk reduction during winter and as such contribute to the erosion protection of the more landward, higher located marsh portions. Our results showed the role of belowground biomass in reducing erosion risks under sandy conditions; however, we could not observe erosion events at sites with finer sediments. These findings especially emphasize the importance of a sequence of marsh developmental stages over the sea-to-land gradient, consisting of a minimal width of low pioneer tidal marshes to ensure the erosion protection and persistence of a high marsh in the more landward direction. Hence, we argue that it is important to have a gradually sloping sea-to-land sequence from tidal flat, over low pioneer tidal marsh, to high marsh, to provide effective nature-based shoreline protection. Future research on the wave attenuation capacity and sediment stability (and other shoreline protection functions such as reduced wave reflection and storm surge attenuation) during the winter period, including the more landward located higher portions of marshes, should give better insights in seasonal changes to predict threshold marsh widths that ensure the shoreline protection function throughout seasons.

Our findings show that nature-based shoreline protection by conserving, restoring, or creating tidal marshes should take into account the seasonal dependency of the protection function of tidal marshes in terms of wave attenuation and erosion reduction. In winter, during the main storm season, wave attenuation rates in pioneer tidal marshes are reduced due to the annual biological cycle of these plants. Management and policy makers should take into account that the width of tidal marshes and a sequence of gradually sloping low to high marshes are crucial to ensure sufficient wave attenuation and by extend, shoreline protection throughout the year.

References

Allison, I., and others. 2009. The Copenhagen diagnosis.

Arkema, K. K., R. Griffin, S. Maldonado, J. Silver, J. Suckale, and A. D. Guerry. 2017. Linking social, ecological, and physical science to advance natural and nature-based protection for coastal communities. Ann. N. Y. Acad. Sci. **1399**: 5–26. doi:10.1111/nyas.13322

Barbier, E. B., and others. 2008. Coastal ecosystem-based management with nonlinear ecological functions and values - supporting material. Science **319**: 321–323. doi:10.1126/science.1150349

Barbier, E. B., S. D. Hacker, C. Kennedy, E. W. Koch, A. C. Stier, and B. R. Silliman. 2011. The value of estuarine and coastal ecosystem services. Ecol. Monogr. **81**: 169–193. doi:10.1890/10-1510.1

Bender, M. A., T. R. Knutson, R. E. Tuleya, J. J. Sirutis, G. A. Vecchi, S. T. Garner, and I. M. Held. 2010. Modeled impact of anthropogenic warming on the frequency of intense Atlantic hurricanes. Science **327**: 454–458. doi:10.1126/science.1180568

Bouma, T. J., M. Friedrichs, B. K. van Wesenbeeck, S. Temmerman, G. Graf, and P. M. J. Herman. 2009. Density-dependent linkage of scale-dependent feedbacks: A flume study on the intertidal macrophyte *Spartina anglica*. Oikos **118**: 260–268. doi:10.1111/j.1600-0706.2008.16892.x

Bouma, T. J., M. B. De Vries, and P. M. J. Herman. 2010. Comparing ecosystem engineering efficiency of two plant species with contrasting growth strategies. Ecol. Soc. Am. **91**: 2696–2704. doi:10.1890/09-0690.1

Bouma, T. J., and others. 2014. Identifying knowledge gaps hampering application of intertidal habitats in coastal protection: Opportunities & steps to take. Coast. Eng **87**: 147–157. doi:10.1016/j.coastaleng.2013.11.014

Carus, J., M. Paul, and B. Schröder. 2016. Vegetation as self-adaptive coastal protection: Reduction of current velocity and morphologic plasticity of a brackish marsh pioneer. Ecol. Evol. **6**: 1579–1589. doi:10.1002/ece3.1904

Charpentier, A., and J. F. Stuefer. 1999. Functional specialization of ramets in *Scirpus maritimus* - splitting the tasks of sexual reproduction, vegetative growth, and resource storage. Plant Ecol **141**: 129–136. doi:10.1023/A:1009825905117

Chen, Y., C. E. L. Thompson, and M. B. Collins. 2012. Saltmarsh creek bank stability: Biostabilisation and consolidation with depth. Cont. Shelf Res. **35**: 64–74. doi:10.1016/j.csr.2011.12.009

Cheong, S.-M., B. Silliman, P. P. Wong, B. van Wesenbeeck, C.-K. Kim, and G. Guannel. 2013. Coastal adaptation with ecological engineering. Nat. Clim. Chang. **3**: 787–791. doi:10.1038/nclimate1854

Christoph Blasi, Axel Winterscheid, and Nathalie CronBundesanstalt für Gewässerkunde. 2014. Sedimentmanagement Tideelbe Strategien und Potenziale -Systemstudie II- Ökologische Auswirkungen der Unterbringung von Feinmaterial. Band 1 (2), Endbericht. Im Auftrag des Wasser- und Schifffahrtsamtes Hamburg. doi:10.5675/BfG-1763

Coops, H., N. Geilen, H. J. Verheij, R. Boeters, and G. Van der Velde. 1996. Interactions between waves, bank erosion and emergent vegetation: An experimental study in a wave tank. Aquat. Bot. **53**: 187–198. doi:10.1016/0304-3770(96)01027-3

Costanza, R., O. Pérez-Maqueo, M. L. Martinez, P. Sutton, S. J. Anderson, and K. Mulder. 2008. The value of coastal wetlands for hurricane protection. Ambio **37**: 241–248. doi:10.1579/0044-7447(2008)37[241:tvocwf]2.0.co;2

Coulombier, T., U. Neumeier, and P. Bernatchez. 2012. Sediment transport in a cold climate salt marsh (St. Lawrence Estuary, Canada), the importance of vegetation and waves. Estuar. Coast. Shelf Sci. **101**: 64–75. doi:10.1016/j.ecss.2012.02.014

Dalrymple, R. A., and R. G. Dean. 1991. Water wave mechanics for engineers and scientists, v. **2**. Prentice-Hall. doi:10.1142/1232

De Baets, S., J. Poesen, B. Reubens, K. Wemans, J. De Baerdemaeker, and B. Muys. 2008. Root tensile strength and root distribution of typical Mediterranean plant species and their contribution to soil shear strength. Plant Soil **305**: 207–226. doi:10.1007/s11104-008-9553-0

Duarte, C. M., I. J. Losada, I. E. Hendriks, I. Mazarrasa, and N. Marbà. 2013. The role of coastal plant communities for climate change mitigation and adaptation. Nat. Clim. Chang. **3**: 961–968. doi:10.1038/nclimate1970

DWD Climate Data Center. 2019. Ftp://Ftp-Cdc.Dwd.de/Pub/CDC/Observations_germany/Climate/Hourly/Pressure/Recent/.

Francalanci, S., M. Bendoni, M. Rinaldi, and L. Solari. 2013. Ecomorphodynamic evolution of salt marshes: Experimental observations of bank retreat processes. Geomorphology **195**: 53–65. doi:10.1016/j.geomorph.2013.04.026

French, J. 2006. Tidal marsh sedimentation and resilience to environmental change: Exploratory modelling of tidal, sea-level and sediment supply forcing in predominantly allochthonous systems. Mar. Geol. **235**: 119–136. doi:10.1016/j.margeo.2006.10.009

Gedan, K. B., M. L. Kirwan, E. Wolanski, E. B. Barbier, and B. R. Silliman. 2011. The present and future role of coastal wetland vegetation in protecting shorelines: Answering recent challenges to the paradigm. Clim. Change **106**: 7–29. doi:10.1007/s10584-010-0003-7

Hjulstrom, F. 1935. Studies of the morphological activity of rivers as illustrated by the River Fyris. Bull. Geol. Inst. Upsalsa **25**: 221–527.

Kappenberg, J., M. Berendt, N. Ohle, R. Riethmüller, D. Schuster, and T. Strotmann. 2016. Seasonal, spring-neap and tidal variation of hydrodynamics and water constituents in the mouth of the Elbe Estuary, Germany. Ocean Sci. Discuss. doi:10.5194/os-2016-7

Kirwan, M. L., and J. P. Megonigal. 2013. Tidal wetland stability in the face of human impacts and sea-level rise. Nature **504**: 53–60. doi:10.1038/nature12856

Kirwan, M. L., S. Temmerman, E. E. Skeehan, G. R. Guntenspergen, and S. Faghe. 2016. Overestimation of marsh vulnerability to sea level rise. Nat. Clim. Chang. **6**: 253–260. doi:10.1038/nclimate2909

Le Hai, T., and H. J. Verhagen. 2014. Damage to grass covered slopes due to overtopping. Coast. Eng. **56**: 21. ISBN 978-0-9896611-2-6.

Leonard, L. A., and A. L. Croft. 2006. The effect of standing biomass on flow velocity and turbulence in *Spartina alterniflora* canopies. Estuar. Coast. Shelf Sci. **69**: 325–336. doi:10.1016/j.ecss.2006.05.004

Ma, Z., T. Ysebaert, D. van der Wal, D. J. de Jong, X. Li, and P. M. J. Herman. 2014. Long-term salt marsh vertical accretion in a tidal bay with reduced sediment supply. Estuar. Coast. Shelf Sci. **146**: 14–23. doi:10.1016/j.ecss.2014.05.001

Möller, I., and others. 2014. Wave attenuation over coastal salt marshes under storm surge conditions. Nat. Geosci **7**: 727–731. doi:10.1038/ngeo2251

Morris, M., M. Hassan, A. Kortenhaus, and P. Visser. 2009. Breaching processes: A state of the art review. FLOODsite Publ. 70. T06-06-03.

Mudd, S. M., A. D'Alpaos, and J. T. Morris. 2010. How does vegetation affect sedimentation on tidal marshes? Investigating particle capture and hydrodynamic controls on biologically mediated sedimentation. J. Geophys. Res. Earth Surf **115**: 1–14. doi:10.1029/2009JF001566

Narayan, S., and others. 2016. The effectiveness, costs and coastal protection benefits of natural and nature-based defences. PLoS One **11**: e0154735. doi:10.1371/journal.pone.0154735

Narayan, S., and others. 2017. The value of coastal wetlands for flood damage reduction in the northeastern USA. Sci. Rep **7**: 1–12. doi:10.1038/s41598-017-09269-z

Nolte, S., E. C. Koppenaal, P. Esselink, K. S. Dijkema, M. Schuerch, A. V. De Groot, J. P. Bakker, and S. Temmerman. 2013. Measuring sedimentation in tidal marshes: A review on methods and their applicability in biogeomorphological studies. J. Coast. Conserv. **17**: 301–325. doi:10.1007/s11852-013-0238-3

R Core Team, R: A Language and Environment for Statistical Computing, Vienna, Austria, 2016.

Silinski, A., E. Fransen, T. J. Bouma, P. Meire, and S. Temmerman. 2016*a*. Unravelling the controls of lateral expansion and elevation change of pioneer tidal marshes. Geomorphology **274**: 106–115. doi:10.1016/j.geomorph.2016.09.006

Silinski, A., and others. 2016*b*. Effects of contrasting wave conditions on scour and drag on pioneer marsh plants. Geomorphology **255**: 49–62. doi:10.1016/j.geomorph.2015.11.021

Silinski, A., K. Schoutens, S. Puijalon, J. Schoelynck, D. Luyckx, P. Troch, P. Meire, and S. Temmerman. 2017. Coping with waves: Plasticity in tidal marsh plants as self-adapting coastal ecosystem engineers. Limnol. Oceanogr. **63**: 799–815. doi:10.1002/lno.10671

Smolders, S., Y. Plancke, S. Ides, P. Meire, and S. Temmerman. 2015. Role of intertidal wetlands for tidal and storm tide attenuation along a confined estuary: A model study. Nat. Hazards Earth Syst. Sci. **15**: 1659–1675. doi:10.5194/nhess-15-1659-2015

Spencer, T., S. M. Brooks, B. R. Evans, J. A. Tempest, and I. Möller. 2015. Earth-science reviews southern North Sea storm surge event of 5 December 2013 : Water levels, waves and coastal impacts. Earth Sci. Rev **146**: 120–145. doi:10.1016/j.earscirev.2015.04.002

Stanczak, G., H. Oumeraci, and A. Kortenhaus. 2007. Laboratory tests on the erosion of clay revetment of sea dike with and without a grass cover induced by breaking wave impact. FLOODsite Publ., **935**, T04-07-11.

Stark, J., T. Van Oyen, P. Meire, and S. Temmerman. 2015. Observations of tidal and storm surge attenuation in a large tidal marsh. Limnol. Oceanogr. **60**: 1371–1381. doi:10.1002/lno.10104

Steendam, G. J., P. Peeters, J. W. van der Meer, K. Van Doorslaer, and K. Trouw. 2011. Destructive wave overtopping tests on Flemish dikes, p. 49–50. *In* International Conference on Coastal Structures 2011, September 5–9, 2011, Yokohama, Japan: Book of abstracts. doi:10.1142/9789814412216_0016

Strotmann, T. 2014. Deutsches Gewässerkundliches Jahrbuch, Elbegebiet Teil 3, Untere Elbe ab der Havelmündung. Freie und Hansestadt Hamburg HPA Hamburg Port Authority AöR: ISSN 0949-3654.

Sutherland, T. F., J. Grant, and C. L. Amos. 1998. The effect of carbohydrate production by the diatom *Nitzschia curvilineata* on the erodibility of sediment. Limnol. Oceanogr. **43**: 65–72.

Sutton-Grier, A. E., K. Wowk, and H. Bamford. 2015. Future of our coasts: The potential for natural and hybrid infrastructure to enhance the resilience of our coastal communities, economies and ecosystems. Environ. Sci. Policy **51**: 137–148. doi:10.1016/j.envsci.2015.04.006

Temmerman, S., P. Meire, T. J. Bouma, P. M. J. Herman, T. Ysebaert, and H. J. De Vriend. 2013. Ecosystem-based coastal defence in the face of global change. Nature **504**: 79–83. doi:10.1038/nature12859

Temmerman, S., and M. L. Kirwan. 2015. Building land with a rising sea: Cost-efficient nature-based solutions can help to sustain coastal societies. Science **349**: 588–589. doi:10.1126/science.aac8312

Tempest, J. A., I. Möller, and T. Spencer. 2015. A review of plant-flow interactions on salt marshes: The importance of vegetation structure and plant mechanical characteristics. Wiley Interdiscip. Rev. Water **2**: 669–681. doi:10.1002/wat2.1103

Turner, R. K., D. Burgess, D. Hadley, E. Coombes, and N. Jackson. 2007. A cost-benefit appraisal of coastal managed realignment policy. Glob. Environ. Chang. **17**: 397–407. doi:10.1016/j.gloenvcha.2007.05.006

van Baars, S., and I. M. van Kempen. 2009. The causes and mechanisms of historical dike failures in The Netherlands. E-WAter: ISSN 1994-8549.

Van Coppenolle, R., C. Schwarz, and S. Temmerman. 2018. Contribution of mangroves and salt marshes to nature-based mitigation of coastal flood risks in major deltas of the world. Estuaries Coast. **41**: 1699–1711. doi:10.1007/s12237-018-0394-7

van Wijnen, H. J., and J. P. Bakker. 2001. Long-term surface elevation change in salt marshes: A prediction of marsh response to future sea-level rise. Estuar. Coast. Shelf Sci. **52**: 381–390. doi:10.1006/ecss.2000.0744

Vannoppen, W., M. Vanmaercke, S. De Baets, and J. Poesen. 2015. A review of the mechanical effects of plant roots on concentrated flow erosion rates. Earth Sci. Rev. **150**: 666–678. doi:10.1016/j.earscirev.2015.08.011

Vannoppen, W., S. De Baets, J. Keeble, Y. Dong, and J. Poesen. 2017. How do root and soil characteristics affect the erosion-reducing potential of plant species? Ecol. Eng. **109**: 186–195. doi:10.1016/j.ecoleng.2017.08.001

Vuik, V., S. N. Jonkman, B. W. Borsje, and T. Suzuki. 2016. Nature-based flood protection: The efficiency of vegetated foreshores for reducing wave loads on coastal dikes. Coast. Eng. **116**: 42–56. doi:10.1016/j.coastaleng.2016.06.001

Vuik, V., H. Y. Suh Heo, Z. Zhu, B. W. Borsje, and S. N. Jonkman. 2018. Stem breakage of salt marsh vegetation under wave forcing: A field and model study. Estuar. Coast. Shelf Sci. **200**: 41–58. doi:10.1016/j.ecss.2017.09.028

Wamsley, T. V., M. A. Cialone, J. M. Smith, J. H. Atkinson, and J. D. Rosati. 2010. The potential of wetlands in reducing storm surge. Ocean Eng. **37**: 59–68. doi:10.1016/j.oceaneng.2009.07.018

Wang, H., D. Van Der Wal, X. Li, and others. 2017. Zooming in and out: Scale-dependence of extrinsic and intrinsic factors affecting salt marsh erosion. J. Geophys. Res. Earth Surf **122**: 1455–1470. doi:10.1002/2016JF004193

Woolf, D., and J. Wolf. 2013. Impacts of climate change on storms and waves. MCCIP Sci. Rev **2013**: 20–26. doi:10.14465/2013.arc03.020-026.

Yang, S. L., B. W. Shi, T. J. Bouma, T. Ysebaert, and X. X. Luo. 2012. Wave attenuation at a salt marsh margin: A case study of an exposed coast on the Yangtze Estuary. Estuaries Coast. **35**: 169–182. doi:10.1007/s12237-011-9424-4

Ysebaert, T., S. Yang, L. Zhang, Q. He, T. J. Bouma, and P. M. J. Herman. 2011. Wave attenuation by two contrasting ecosystem engineering salt marsh macrophytes in the intertidal pioneer zone. Wetlands **31**: 1043–1054. doi:10.1007/s13157-011-0240-1

Acknowledgments

We would like to thank Wasserstraßen- und Schifffahrtsamt Hamburg (Glückstadt, Germany) for logistical support in the field; Elmar Fuchs for valuable discussion; Flanders Hydrology for providing the Matlab routine to process the wave data and all field assistants for occasional help. This research was financed by the research project TIBASS (Tidal Bank Science and Services) of the Bundesanstalt für Gewässerkunde (Bfg), Koblenz and the Research Foundation Flanders (FWO, PhD grant K. Schoutens, 1116319N).

Conflict of Interest

None declared.

Submitted 22 May 2018
Revised 26 November 2018
Accepted 31 January 2019

Associate editor: Luiz Drude de Lacerda